# Performance of Nozzle Steels in Biofuel[a]

## Evaluación del comportamiento de aceros de toberas aceros de toberas en biocombustible

Received: August 08, 2020 | Accepted: June 16, 2021 | Published: July 27, 2022

**David Leonardo Blanco-Estupiñan***
Escuela Colombiana de Ingeniería Julio Garavito, Bogotá, Colombia
ORCID: https://orcid.org/0000-0002-8114-4764

**Angela Bermudez-Castañeda**
Escuela Colombiana de Ingeniería Julio Garavito, Bogotá, Colombia
ORCID: https://orcid.org/0000-0002-3766-2695

**Sebastian Márquez**
Escuela Colombiana de Ingeniería Julio Garavito, Bogotá, Colombia
ORCID: https://orcid.org/0000-0002-4120-6051

[a] Research paper (Artículo de investigación) - Article of scientific and tecnological investigation

* Corresponding author. E-mail: david.blanco@escuelaing.edu.co

DOI: https://doi.org/10.11144/javeriana.iued26.pnsb

**How to cite this article:**
A. Bermudez-Castañeda, D. L. Blanco-Estupiñan, S. Márquez, "Performance of Nozzle Steels in Biofuel" Ing. Univ. vol. 26, 2022. https://doi.org/10.11144/javeriana.iued26.pnsb

## Abstract

***Objective:*** To evaluate the corrosion resistance of stainless-steel injection nozzles under immersion test in biodiesel and perform electrochemical characterization under $HNO_3$ solutions. ***Methods and materials:*** Chemical characterization of biofuel was performed to analyze its stability. Immersion tests were carried out for 4 months, evaluating 304 stainless steel under 3 different diesel/biofuel mixtures concentrations. Additionally, polarization tests were done using NOx concentrations above the levels measured from engine emissions. ***Results and discussion:*** The use of biofuels in Colombia has been largely driven by ethanol production from vegetable sources. Their use brings some advantages related to reducing emissions of particles and toxic gases (mainly aromatic groups, NOx, and CO2). However, degradation of materials can occur when they are in direct contact with biodiesel. Furthermore, solidification into waxes, which leads to plugging of nozzles, has been reported. However, it is unknown whether this influences oxygen diffusion in the solution and, in turn, affects the corrosion resistance of stainless steel. ***Conclusions:*** The corrosion resistance of the 304 stainless steel changed under immersion conditions, even though its protective layer was not affected by the NOx concentrations registered in the biofuel mixtures.


**Keywords:** biofuel, nozzle, stainless steel.


## Resumen

***Objetivo:*** evaluar la resistencia a la corrosión de las boquillas de inyección de acero inoxidable bajo ensayo de inmersión en biodiésel, y realizar una caracterización electroquímica bajo soluciones de $HNO_3$. ***Métodos y materiales:*** Se realizó la caracterización química del biodiésel para analizar su estabilidad. Se realizaron pruebas de inmersión durante 4 meses, evaluando el acero inoxidable 304 bajo 3 concentraciones diferentes de mezclas de diésel/biocombustible. Además, se realizaron ensayos de polarización con concentraciones de NOx superiores a los niveles medidos en las emisiones de los motores. ***Resultados y discusión:*** El uso de biocombustibles en Colombia ha sido impulsado en gran medida por la producción de etanol de origen vegetal. Su uso aporta algunas ventajas relacionadas con la reducción de las emisiones de partículas y gases tóxicos (principalmente, grupos aromáticos, NOx y CO2). Sin embargo, puede producirse una degradación de los materiales cuando están en contacto directo con el biodiésel. Además, se ha informado de solidificación de ceras, que provoca el taponamiento de las boquillas. No obstante, se desconoce si esto influye en la difusión del oxígeno en la solución y, a su vez, afecta a la resistencia a la corrosión del acero inoxidable. ***Conclusiones:*** La resistencia a la corrosión del acero inoxidable 304 cambió bajo condiciones de inmersión, aunque su capa protectora no se vio afectada por las concentraciones de NOx registradas en las mezclas de biocombustible.


**Palabras clave:** bicombustible, toberas, acero inoxidable.

## Introduction

Stainless steels are widely used in various industrial applications, which include very aggressive environments. This has influenced the development and study of their properties, which strongly impact the service life of components and equipment [1]. In particular, the automotive industry uses a wide range of parts made from stainless steel. This is particularly the case for combustion systems, where mechanical and chemical stabilization properties play a crucial role in the nozzles' performance and the low-pressure systems in contact with fuel.

Metals used for automobile production, such as copper, aluminum, and cast iron, are highly resistant to corrosion when immersed in diesel fuel. However, they suffer more accelerated corrosion processes when in contact with biodiesel and mixtures. Therefore, to extend the lifespan of these metals, the study of the corrosive nature of biodiesel is important [2]. This is particularly so given the advantages of biodiesel, which have led to a worldwide increase in its use. The main advantages of biodiesel are its low Sulphur content and the fact that it does not involve burning fossil fuels, given the current environmental crisis.

Biofuels extracted from vegetable sources have significantly different in particulate matter emissions and biodegradability compared to conventional biodiesel. Currently, the diesel fuel distributed and used in Colombia contains around 10% particulate matter [3].

Considering the above, this work focuses on studying the corrosion resistance of AISI 304 stainless steel, the type used in commercial nozzles, when exposed to pure biodiesel fuel and its mixture B50 (50% palm oil, 50% commercial diesel) under stationary immersion conditions. In order to separate the influence of the NOx species, potentiostatic polarization tests were done under concentrations of 0.1M, 1x10-3M, and 1x10-4M.

Under stationary immersion conditions, biodiesel suffered solidification, manifesting in the formation of wax, as reported in the literature [4]. This could restrict or reduce the use of mixtures with a high percentage of biofuels in locations with cold weather (<18°C). Furthermore, localized corrosion was observed on the nozzles, even though no degradation was observed under the electrochemical test, suggesting that the corrosion was caused by oxygen depletion.

# Materials and methods

## Preparation of the samples

Commercial nozzles were used for the immersion tests, along with AISI 304 rod, a common material used for nozzles. The nozzles were degreased in a basic solution and rinsed with distilled water. Later, they were subjected to ultrasonic cleaning in ethanol for 30 minutes. Once the nozzles were dry, they were subjected to the immersion test. Before performing the electrochemical tests, the same procedure was used to clean an AISI 304 disk cut from the rod.

## Biodiesel Characterization

Commercial biodiesel samples were obtained and mixed with commercial diesel for the immersion test. However, pure biodiesel properties were analyzed according to THE tests described in Table 1.

**Table 1. Tests of the descriptions of the fuel**

| Test | Regulation |
|---|---|
| Biofuel content | EN 14078 |
| Viscosity at 40°C | ASTM D 445 |
| Oxidation stability (Rancimat) | EN 14112-EN 15751 |
| Iodine value | EN 14111 |
| Acid number | ASTM D664 |
| Free glycerin monoglycerides, diglycerides, triglycerides, total glycerin | ASTM D6584 |

**Source: Own source**

## Stainless steel performance under total immersion in biofuel

The stainless-steel nozzles and the AISI 304 disks were subjected to stationary immersion tests for 4 months. Solutions used in the tests were 100% biodiesel and a mixture of biofuel (50%) and commercial diesel (50%). This proportion was taken from a previous study, where the effect of different mixtures on the efficiency of engine combustion was analyzed [5]. In all cases, the samples were covered by biodiesel or the mixture. The environmental temperature was measured, obtaining a range between 14ºC and 20ºC.

## Electrochemical description of the stainless steel in biofuel

NOx emission measurements were taken from the combustion of biodiesel in a test engine to measure the concentration of those species in the biofuel. The value recorded for parts per million was taken as the lower concentration in the electrolyte used to perform potentiostatic tests carried out in an Autolab 305 potentiostat. A standard 3 electrode cell was used, composed of an Ag/AgCl reference electrode, a platinum counter electrode, and a disk made of AISI 304 as a work electrode. $HNO_3$ solutions with concentrations of 0.1M, $1x10^{-3}$M, and $1x10^{-4}$M were used as electrolytes. The polarization curves were carried out between -1V and 1V.

## Results

### Biofuel Chemical characterization

In general, to determine the main properties of biofuels and their mixtures, the biodiesel volume fraction in the mixture is considered and reported [6]. Modern diesel engines can use pure biofuel (B100) or mixtures with diesel petrol [7]. In addition to being extracted from renewable sources, biodiesel offers several advantages: it is biodegradable, non-toxic, reduces toxic emissions, and is ecofriendly when mixed with diesel fuel [8]. Nevertheless, biodiesel has some negative aspects, such as oxidative instability, poor/low-temperature properties, and similar properties to solvents. It can also provide slightly low power and torque and, therefore, higher fuel consumption [9]. Given this, chemical characterization was performed to determine the stability and oxidative properties of the biofuel used.

The viscosity of biodiesel depends mainly on the biofuel chain composition and unsaturation, as well as on its temperature. An acceptable range for the kinematic viscosity can be between 1.9 and 6 $mm^2/s$, according to ASTM D6751 [10]. The biodiesel kinematic viscosity was determined following the procedure described by ASTM D445 [11]. Values around 4.43 $mm^2/s$ were obtained. Although this value is within the acceptable range, it is localized around the mean. This can be explained by a higher number of double links [12].

Likewise, the acid value measurements were done under the procedure described by ASTM D664 [13], where the amount of potassium hydroxide reactive needed to neutralize 1 gram of methyl ester is determined [12]. According to ASTM D6751, the acid value could reach a maximum of 0.5 mg KOH/g of biodiesel [10]. The biodiesel reached a value of 0.23 mg KOH/g, meaning that it has low or no significant corrosion effects on the materials in contact with it. Thus, higher biofuel acid values lead to greater corrosive effects.

Finally, chemical stability was also determined using the iodine value, the maximum of which is around 120gI/100g [12]. The value obtained following the procedure explained in EN 14111 [14] was 59.3gI/100g. Furthermore, triglycerides were detected, implying a complete transformation of the starting composites. In turn, diglycerides and linked glycerin were identified as the main components in mass percentage (w/w).

## Chemical composition of commercial nozzles

The chemical composition, described in Table 2, was obtained according to the procedure explained in ASTM A570 [15]. The atomic percentages identified correspond to UNS S3020 type 302 stainless steel.

**Table 2. Commercial nozzles composition**

| Element | Weight percentage (%) |
|---|---|
| Carbon | 0.091 |
| Silica | 0.452 |
| Manganese | 1.350 |
| Chrome | 17.640 |
| Molybdenum | 0.549 |
| Nickel | 8.110 |
| Phosphorus | 0.0358 |
| Sulphur | 0.0231 |

**Source: Own source**

## Chemical composition of stainless-steel disks

Chemical composition of the sample disks is shown in Table 3. This corresponds to UNS S30400 type 304 stainless steel. The characterization test was done under the procedure described in ASTM A570 [15].

**Table 3. Stainless-steel disk composition.**

| Element | Weight percentage (%) |
|---|---|
| Carbon | 0.0708 |
| Silica | 0.446 |
| Manganese | 1.55 |
| Chrome | 18.22 |
| Molybdenum | 8.36 |
| Nickel | 0.0323 |
| Phosphorus | 0.0221 |

**Source: Own source**

## Hardness measurements of nozzles

Hardness values, shown in Table 4, were obtained according to ASTM E 18 – 03 [16]. As observed, the variability of those values is not significant. This may correspond to hardening due to the cold work done during the manufacturing process.

**Table 4. Commercial nozzles hardness**

| Rockwell (HRb) hardness | |
|---|---|
| Nozzle 1 | 90.53 |
| Nozzle 2 | 91.02 |
| Nozzle 3 | 92.46 |

**Source: Own source**

## Static Immersion tests

Static immersion tests and mass loss control were carried out according to the procedure described in ASTM G31 – 72 [17]. The AISI 304 stainless steel disks and commercial nozzles were evaluated over 154 days (approximately 3696 hours) in B50 and commercial diesel under temperatures from 14ºC-18ºC, humidity (80% HR), and controlled static conditions.

As observed in Figures 1a and 1b, a solid wax or deposits were formed. As reported in previous studies [18], this wax is produced by separating biodiesel components below 13ºC. However, these waxes appear around 16ºC, which can obstruct the injector nozzles in cities where the environmental temperature can reach relatively low values, such as Bogotá.

**Figure 1. Immersion tests**

**(a) Stainless steel disks** **(b) Commercial nozzles**

**Source: Own source**

Once the test was finished, rust and deposits were observed in the commercial diesel fuel and the B50. Moreover, localized corrosion was found inside the nozzle, as shown in Figure 2b. This degradation mechanism is attributed to oxygen depletion, which could occur because of a static solution's decrease in oxygen evolution. The lack of oxygen affects the integrity of the stainless-steel passive layer. This phenomenon was found only under static immersion conditions.

**Figure 2. Nozzles visual inspection.**

**(a) Before immersion** **(b) After immersion**

**Source: Own source**

Likewise, the AISI 304 stainless steel disks were subjected to immersion conditions. However, because of the ease of handling of the samples, metallographic analysis was performed before and after the test.

Three samples were prepared according to ASTM E3–01 [19]. In order to identify the microstructure, samples were chemically attacked for19 minutes with a solution composed of 5ml of HCl, 1 g of picric acid, and 100 ml of ethanol. The procedure was done following ASTM E407–07 [20]. The microstructure was confirmed by duplicated samples.

**Figure 3. Micrographics before the immersion**

**(a) 100x** **(b) 500x**

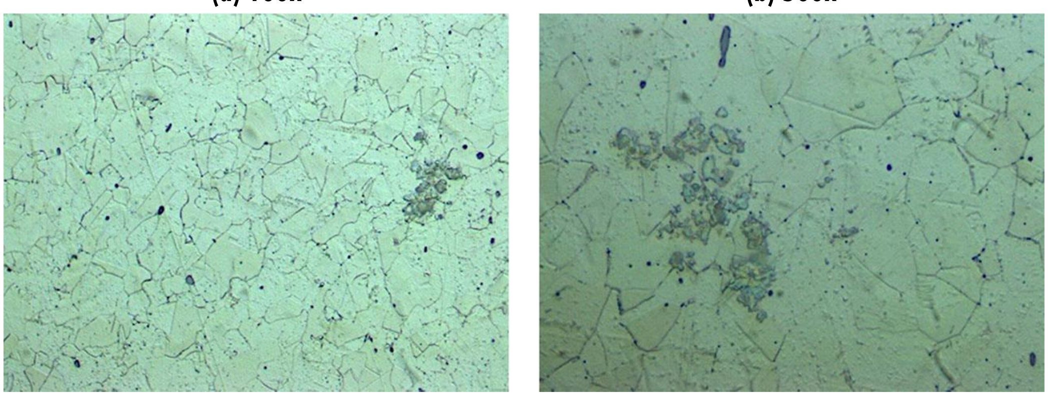

**Source: Own source**

The metallographic characterization shows an austenite matrix in the equi–axial grains of austenite with the presence of carbon (black zone), as seen in Figures 3a and 3b. This microstructure was corroborated using the *metallographic handbook* of the ASM [21]. No evidence of changes in the microstructure was noticed, as observed in Figures 4a and 4b.

**Figure 4. Micrographics after the immersion test.**

**(a) 100x** **(b) 500x**

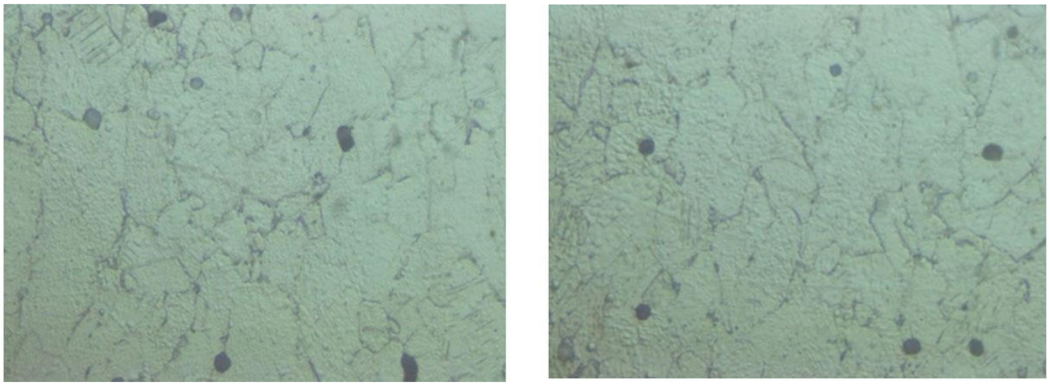

**Source: Own source**

## Electrochemical description of the stainless steel in the biofuel

As the identification of composites rich in N from biodiesel mixtures is challenging, some reference values of the emissions were considered to determine the range of NOx species that can be in contact with the biodiesel. Gas emissions measurements were done from the combustion by-products of an engine where a mixture of diesel and biodiesel was used. The efficiency of the engine and the combustion characteristics are reported elsewhere [22].

Figure 5a and 5b show the NOx content in the combustion gases for the different mixtures used. In all cases, such emissions are below 500 parts per million (ppm), corresponding to concentrations around $1x10^{-3}$M and $1x10^{-4}$M $HNO_3$. Polarization tests were done under those concentrations and 0.1 M $HNO_3$. The last of these was used to compare results from $1x10^{-3}$M and $1x10^{-4}$M $HNO_3$.

**Figure 5. Measurements of NOx emission during combustion**

**(a) B10** **(b) B50**

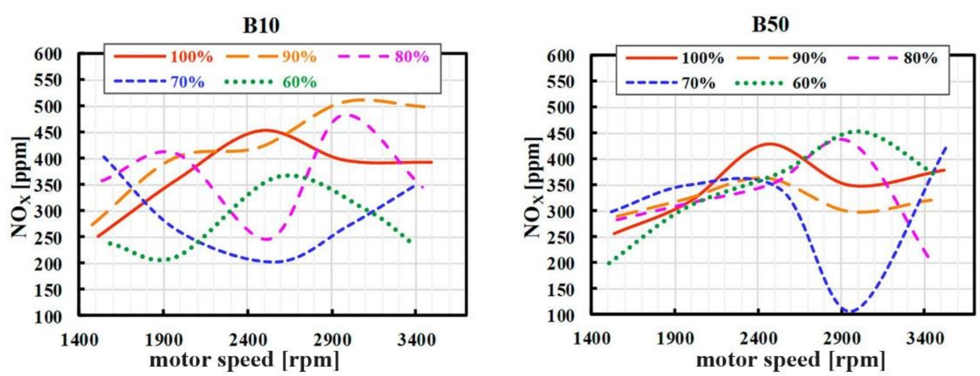


**Source: Own source**

As shown in Figures 6a, 6b, and 6c, no significant variation in corrosion speed or in the passive behavior of the AISI 304 stainless steel was observed.

**Figure 6. polarization curves of the Inox 304 steel.**
**(a) 0.1M. (b) 1 x $10^{-3}$ M. (c) 1 x $10^{-4}$ M**

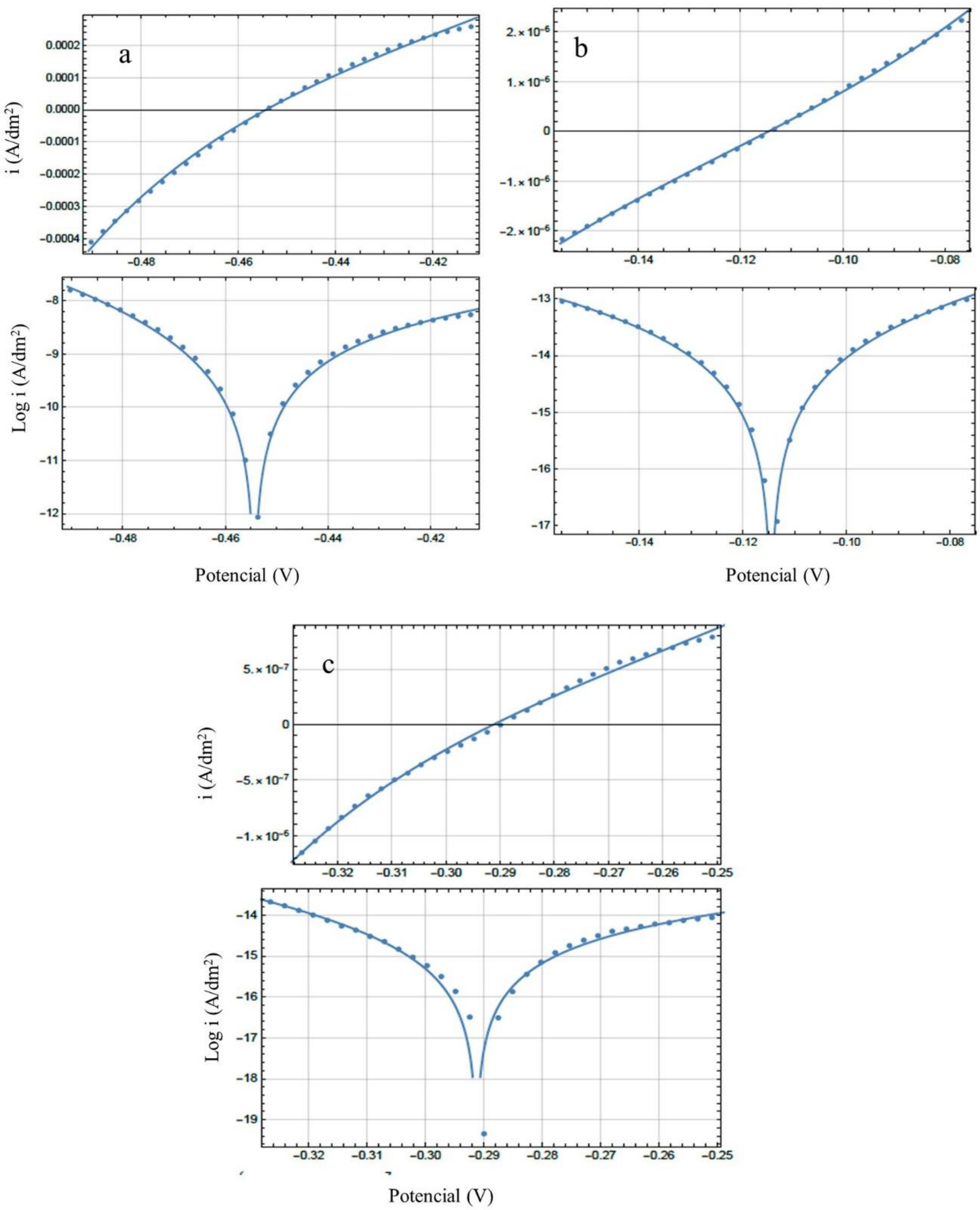


**Source: Authors own creation**

The highest corrosion speeds are associated with the material exposed to the 0.1M $HNO_3$ solution. This is observed in the corrosion parameters, as the corrosion current (icorr) and corrosion potential (Ecorr) are lower for concentrations under $1x10^{-3}$M and $1x10^{-4}$M, as shown in Table 5. This means that the corrosion potential occurs at higher potentials. Likewise, the corrosion current (icor) for 0.1M $HNO_3$ has two higher magnitudes than the other two concentrations. However, from the electrochemical test, it can be concluded that a greater proportion of the NOx species can lead to the potential corrosion displacement and drive the system to faster passivation of the stainless steel, as has been reported in some other research studies on 300 series stainless steel [23, 24].

**Table 5. Polarization curves data of stainless steel in different concentrations of $HNO_3$**

| [$HNO_3$] (M) | icorr | Ecorr |
|---|---|---|
| 0,1 | 2 E-04 | -0,45 |
| $1x10^{-3}$ | 1.3E-06 | -0.12 |
| $1x10^{-4}$ | 6.1E-07 | -0.29 |

**Source: Own source**

In addition, complete polarization curves performed under concentrations of 0.1M and $1x10^{-3}$M $HNO_3$ (Figure 7), show the Ecorr displacement mentioned above. Differences in the current could be related to ohmic fall, as the test was done without a supporting electrolyte to improve conductivity. The analyzed surface did not show localized corrosive phenomena in all cases because the material did not reach the breakdown potentials.

**Figure 7. Comparison of the polarization curve at different concentrations of $HNO_3$**

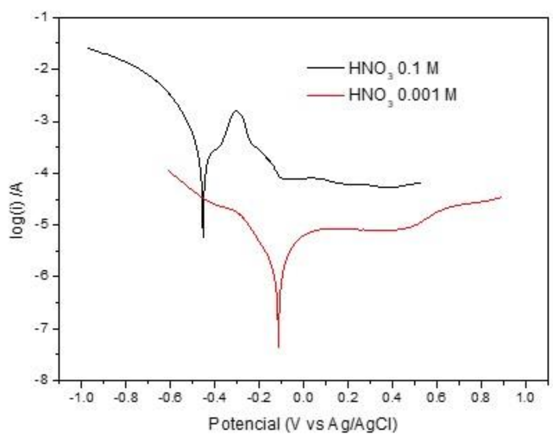


**Source: Own source**

The passive layer peak formation was not observed under low concentrations ($1x10^{-3}$M $HNO_3$), as shown in the polarization curve performed under 0.1M $HNO_3$. This is attributed to the passive layer formation being reached under lower potentials, which means the passive layer is more stable under this concentration.

## Conclusions

- Biodiesel extracted from plant oil shows stability and a low tendency to oxidation. The components of this biofuel are mainly diglycerides and linked glycerin.
- Under immersion, the commercial nozzles exhibited localized corrosion due to aeration of differential cells formed under static conditions.
- After three months of immersion, the AISI 304 stainless steel does not show significant metallographic changes. Differences in the attacked surface between the AISI 304 samples and the commercial nozzles can be explained by the difference in their chemical composition.
- Wax was formed around 16ºC. This can lead to obstruction of the nozzles when higher concentrations of biodiesel are used in the mixture fuel.
- According to corrosion tests, the NOx concentration of the biodiesel does not affect the passive layer or the self–protective performance of the steel.
- The equivalent concentrations of NOx species from the biodiesel show low corrosion potential and corrosion current, which means lower corrosion speeds. Furthermore, no degradation phenomena were identified under any of the concentrations of $HNO_3$ used.

## References

[1] A. Iversen, *Sheir's Corrosion*, 1st ed., Elsevier Science, 2010.

[2] S. Deshpande, A. Joshi, S. Vagge and N. Anekar, "Corrosion behavior of nodular cast iron in biodiesel blends", *Eng. Fail. Anal.*, vol. 105, pp. 1319-1327, 2019, https://doi.org/10.1016/j.engfailanal.2019.07.060

[3] F. Anguebes-Franseschi et al., "Physical and Chemical Properties of Biodiesel Obtained from Amazon Sailfin Catfish (Pterygoplichthys pardalis) Biomass Oil," *Journal of Chemistry*, vol. 2019, p. 7829630, ene. 2019, https://doi.org/10.1155/2019/7829630

[4] E. C. Zuleta, L. Baena, L. A. Rios and J. A. Calderón, "The oxidative stability of biodiésel and its impact on the deterioration of metallic and polymeric materials: a review," *Journal of the Brazilian Chemical Society*, vol. 23, no. 12, pp. 2159-2175, 2012, https://doi.org/10.1590/S0103-50532012001200004

[5] J. Agudelo, E. Gutiérrez y P. Benjumea, "Análisis experimental de la combustión de un motor diésel de automoción operando con mezclas diésel-biodiésel de palma" *Dyna*, vol. 76, no. 159, p. 103-113, 2009.

[6] P. Benjumea and J. Agudelo, "Basic properties of palm oil biodiesel – diesel blends," vol. 87, no. 10-11, pp. 2069-2075, 2008, https://doi.org/10.1016/j.fuel.2007.11.004

[7] S. Lebedevas and A. Vaicekauskas, "Research into the application of biodiesel in the transport sector of Lithuania", Transport, vol. 21, no. 2, pp. 80-87, 2006, https://doi.org/10.3846/16484142.2006.9638047

[8] G. Knothe, "'Designer' Biodiesel: Optimizing Fatty Ester Composition to Improve Fuel Properties," *Energy & Fuels*, vol. 22, no. 2, pp. 1358-1364, 2008. https://doi.org/10.1021/ef700639e

[9] A. Demirbas, "Progress and recent trends in biofuels," *Progress in Energy and Combustion Science*, vol. 33, no. 1, pp. 1-18, 2007, https://doi.org/10.1016/j.pecs.2006.06.001

[10] ASTM D6751-15 International, Standard Specification for Biodiesel Fuel Blend Stock (B100) for Middle Distillate Fuels, 2020.

[11] ASTM D445-17 International, Standard Test Method for Kinematic Viscosity of Transparent and Opaque Liquids (and Calculation of Dynamic Viscosity), 2019.

[12] S. García-Muentes, F. Lafargue Perez, B. Labrada, M. Díaz and A. Campo-Lafita, "Propiedades fisicoquímicas del aceite y biodiesel producidos de la Jatropha curcas L. en la provincia de Manabí, Ecuador" *Revista Cubana de Química*, vol. 30, pp. 142-158, abr. 2018.

[13] ASTM D664-18 International, Standard Test Method for Acid Number of Petroleum Products by Potentiometric Titrationel Blend Stock (B100) for Middle Distillate Fuels, 2018.

[14] UNE EN 14111, Fat and oil derivatives. Fatty Acid Methyl Esters (FAME). Determination of iodine value, 2003.

[15] ASTM A570-98 International, Standard Specification for Steel, Sheet and Strip, Carbon, Hot-Rolled (Withdrawn 2000), 1998.

[16] ASTM E18-03, Standard Test Methods for Rockwell Hardness and Rockwell Superficial Hardness of Metallic Materials, 2003.

[17] ASTM G31-72 International, Standard Practice for Laboratory Immersion Corrosion Testing of Metals, 2004.

[18] G. Dwivedi and M. Sharma, "Impact of cold flow properties of biodiesel on engine performance", *Renew. Sustain. Energy Rev.*, vol. 31, pp. 650-656, 2014.

[19] ASTM E3-01 International, Standard Guide for Preparation of Metallographic Specimens, 2001.

[20] ASTM E407-07 International, Standard test methods for microetching, 2007.

[21] G. F. Vander Voort et al., "ASM handbook", *Metallogr. Microstruct.*, vol. 9, pp. 44073-0002, 2004.

[22] O. H. Venegas and L. F. Mónico, "Estudio de la influencia del uso de combustibles alternativos en un motor de combustión interna", Escuela Colombiana de Ingeniería Julio Garavito, Bogotá D. C:, Informe de investigación, 2019.

[23] D. Kolman, D. Ford, D. Butt and T. Nelson, "Corrosion of 304 stainless steel exposed to nitric acid-chloride environments", *Corros. Sci.*, vol. 39, no. 12, pp. 2067-2093, 1997. https://doi.org/10.1016/S0010-938X(97)00092-9

[24] K. Ishimi, Y. Ida, F. Tsutaka and Y. K. Sugimoto, "Nitric Acid Passivation Treatment of Type 304 Stainless Steels with Different Surface Polishing Conditions and Changes in Pitting Inhibition Effect of The Treatment with Exposure to Corrosion Environments", *J. Surf. Finish. Soc. Jpn.*, vol. 66, no. 4, pp. 158-164, 2015, https://doi.org/10.4139/sfj.66.158